

# Exploring the Propagation of the Madden-Julian Oscillation across the Maritime Continent

Midshipman 1/C Casey R. Densmore

Advisor: Professor Bradford S. Barrett, Oceanography Department, Advisor: CAPT Elizabeth R. Sanabia, Oceanography Department

External Collaborator: Assistant Professor Pallav Ray, Florida Institute of Technology

**Trident Research Objective:** Better understand atmospheric conditions which favor MJO eastward propagation through the Maritime Continent

## Introduction

The Madden-Julian Oscillation (MJO, Madden and Julian 1971) is the leading intraseasonal mode of atmospheric variability. The MJO consists of a broad circulation cell approximately 10,000 km in horizontal extent (Fig. 1; Madden and Julian 1994) that propagates eastward along the equator circumnavigating the globe in the tropics (Zhang 2005) over a period of approximately 30 to 60 days.

MJO circulation (Figs. 1,2) includes:

- Upward motion ("active envelope")
  - Above-normal thunderstorm activity due to upward vertical motion, causing above-average precipitation and wind
- Downward motion ("suppressed envelope")
  - Below-normal thunderstorm activity due to downward vertical motion, causing below average precipitation and wind

Quantifying the MJO

The Wheeler-Hendon Realtime Multivariate (RMM) MJO index (Wheeler and Hendon 2004; WH04) uses wind and outgoing longwave radiation (OLR) to quantify MJO (Fig. 4):

- Geographic location: one of eight phases
- Strength: Active or inactive based on strength of thunderstorm and wind anomalies.

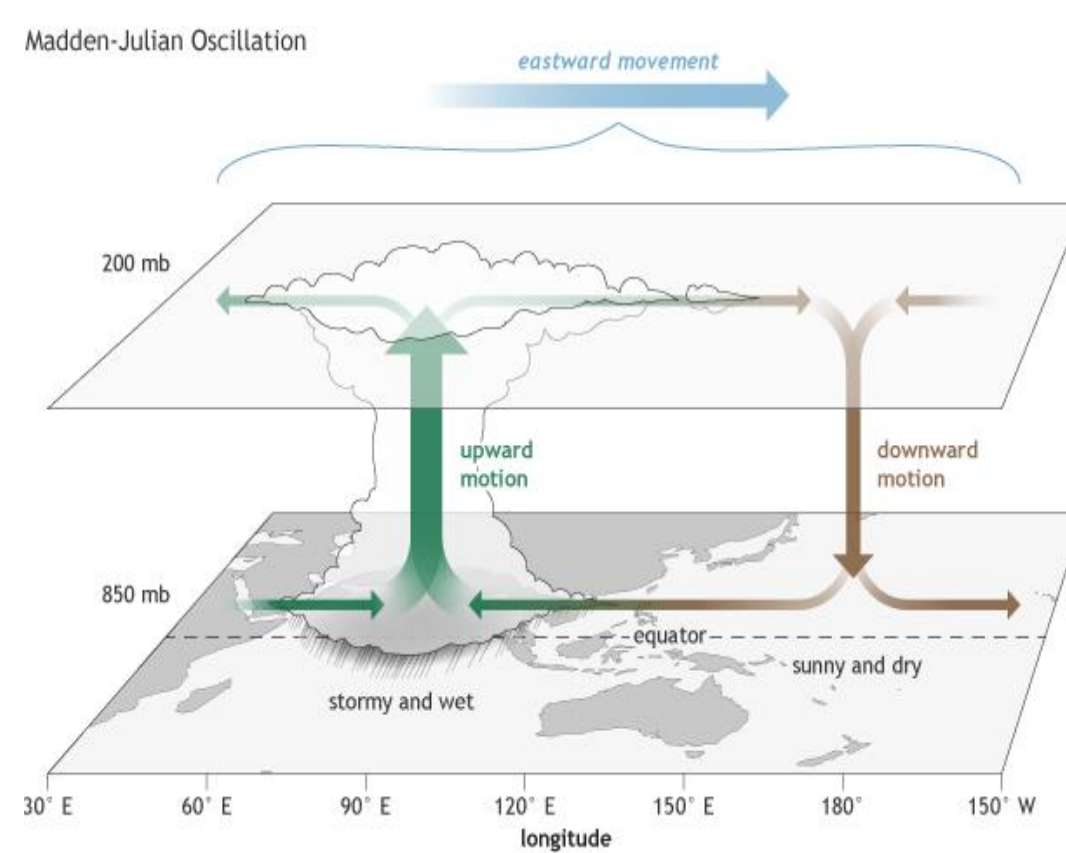


Figure 1: Atmospheric circulation and resultant convective activity typical of the MJO. 2014 NOAA graphic by Fiona Martin.

## Data and Methods

### Classifying MJO Events

- The RMM Index was used to categorize MJO events based on location and strength
  - Categorized as one of four cases based on MJO activity on entrance to and exit from the Maritime Continent (Fig. 4, matching Fig. 2).
  - Eastward propagation required for 65% of days over the MC
- Analysis was repeated for:
  - OLR MJO (OMI) index to confirm results (not shown)
  - Summer with BSISO index to better capture different summer thunderstorm activity
  - MJO events over the Indian Ocean (phases 2 and 3) and western Pacific Ocean (phases 6 and 7) to compare to MC characteristics.
- Analysis was modified to study relationships between MJO amplitude changes over MC and phase of the QBO
  - Mean amplitude changes over the MC for all AA and AI MJO events were compared by QBO phase

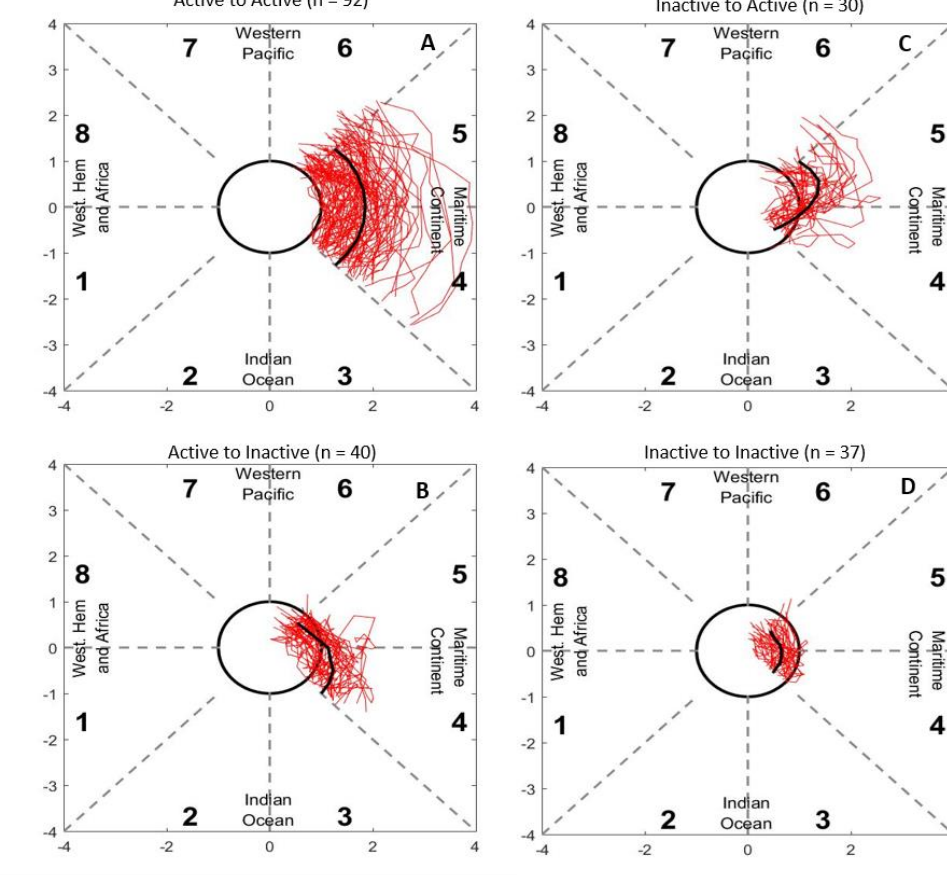


Figure 4: MJO events over the Maritime Continent from 1980-2015 classified as one of four cases by phase 4 and 5 RMM amplitudes: Active-Active (AA, A), Active-Inactive (AI, B), Inactive-Active (IA, C), and Inactive-Inactive (II, D). Black lines denote average amplitudes for all MJO events of each case.

## Result: Background Atmospheric States

**Primary Result 1:** Increased moisture and lower pressures are potential precursors for MJO propagation regardless of initial strength. A more intense lower tropospheric moisture foot east of the active envelope also indicates likely MJO propagation for initially active events. These atmospheric anomalies may provide a predictive capability to detect changes in the MJO prior to those changes projecting on the RMM index.

### Specific Humidity

- AA MJO events are significantly more moist throughout the troposphere in the active envelope than AI events from days -8 to +8 (Figs. 7C,F,I)
- Positive low-level humidity (moisture foot) extends eastward over the MC at day 0
  - Signature is significantly more moist for AA events than AI events (Fig. 7F)
  - No moisture foot signature present for MJO events over the IO or WP (not shown)
- Positive humidity anomalies facilitate enhanced convective development which would enhance MJO propagation

### Geopotential Heights

- Negative low-level and positive upper-level geopotential height anomalies larger for AA events than AI events by day 0 (Fig. 7F),
- Corresponds to lower surface pressure, and faster upward vertical motion for AA events
- Larger geopotential height anomalies enhance circulation in the active envelope thereby strengthening the overall MJO circulation.

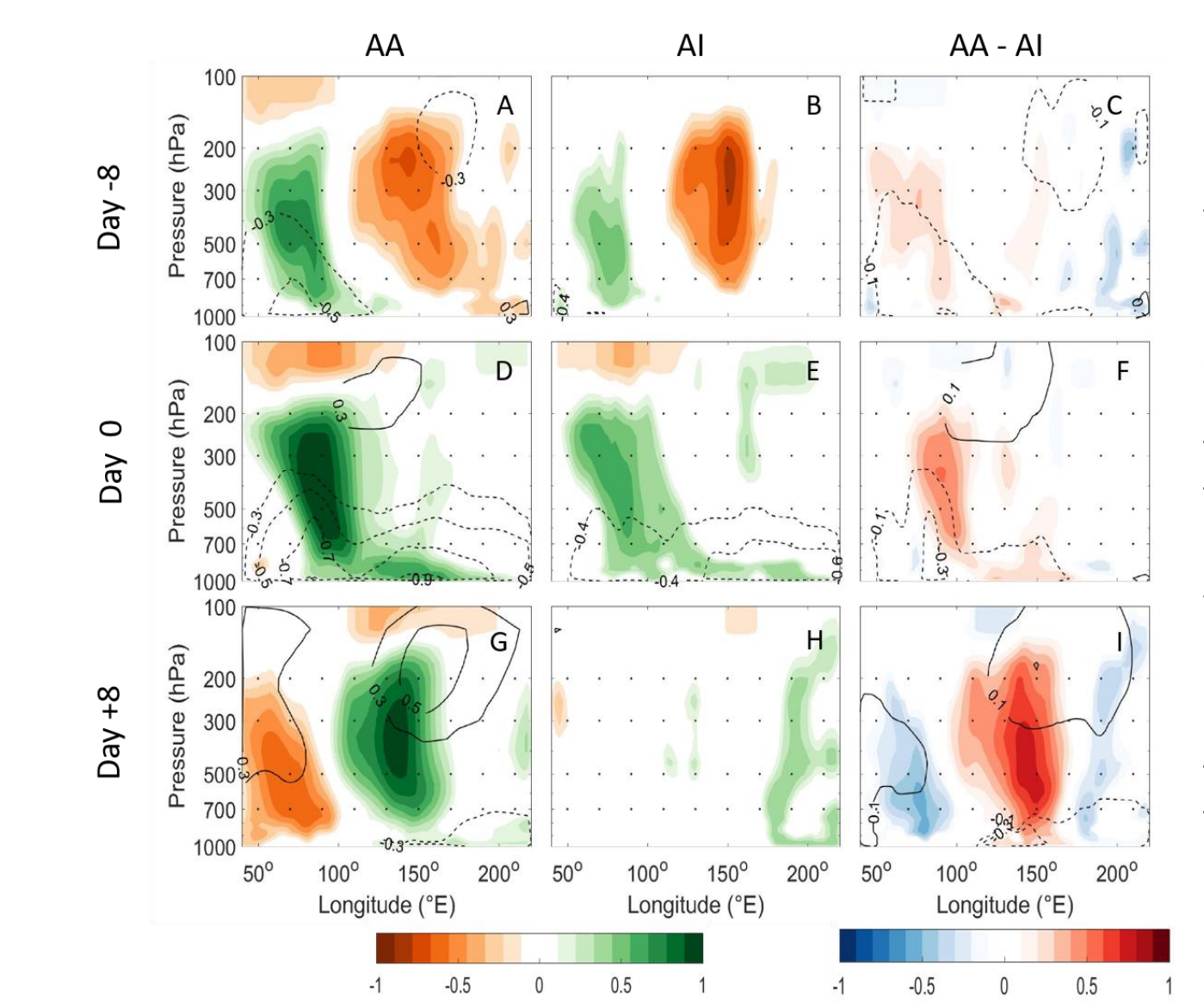


Figure 7: Specific humidity (color-filled) and geopotential height (unfilled) contours, positive represented by solid lines) standard anomaly contours averaged from 15°S to 15°N as the MJO active envelope crosses the western boundary of the MC (100°E). Anomalies are shown for AA (A, D, G) and AI (B, E, H) MJO events, as well as the differences between the two (C, F, I) at -8 (A-C), 0 (D-F), and 8 (G-I) days relative to MJO active envelope entrance to the MC.

### Calculating Anomalies of Background Atmospheric States

- Daily values of specific humidity ( $q$ ) and geopotential heights ( $\phi$ ) from the ERA-Interim Reanalysis were compared among the four MJO cases at 0000 and 1200 UTC from 1980-2015.
- Standard anomalies were calculated following Eq. 1, where:
  - $q$  is the parameter analyzed,  $\mu$  is the climatological monthly mean from 1980-2015, and  $\sigma$  is the standard deviation of the monthly mean
- Statistical significance was tested at the 95% confidence level

$$q_{stdanom_i} = \frac{q_{i,j} - \mu_j}{\sigma_j} \quad (1)$$

### Quantifying the QBO with an EOF analysis

- EOF analysis of global stratospheric zonal winds from 1980-2017 (data from ERA-Interim, Dee et al., 2011)
- Averaged meridionally from 10°S to 10°N
- Bounded vertically by 10 hPa and 100 hPa
- Most variance is captured by the first two PCs in the 2-3 year time period (Fig. 5)

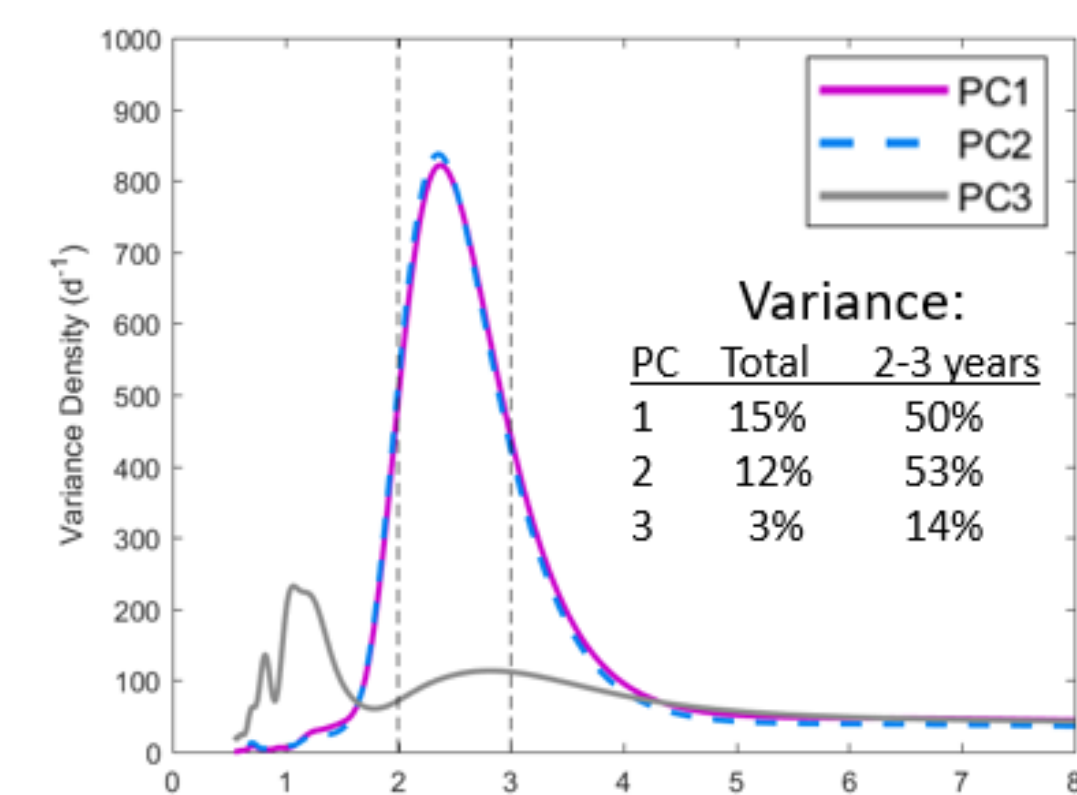


Figure 5: Variance density spectra of the first three principal components.

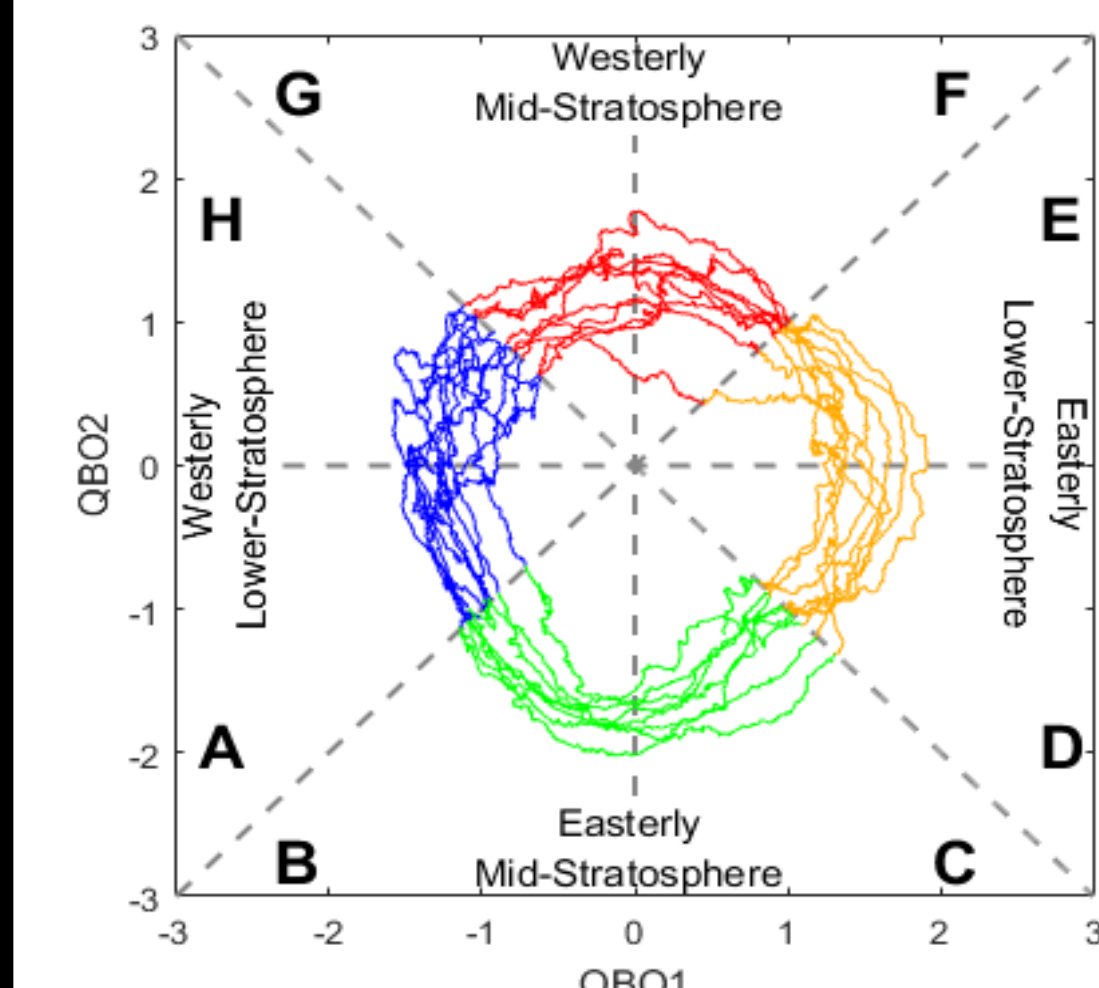


Figure 6: EOF phase space diagram of QBO1 and QBO2 from 1980-2017. Eight phases (separated by dashed lines) divide the QBO zonal winds by direction and altitude of the wind maxima.

Phase space diagram (Fig. 6) shows QBO wind speed and height:

- Angle around center corresponds to altitude, direction of winds
- Radius from center corresponds to wind speed
- QBO winds can be categorized by zonal wind direction and height as one of four phase pairs:
  - QBOWL: Westerly lower-stratospheric winds
  - QBOEM: Easterly mid-stratospheric winds
  - QBOEL: Easterly lower-stratospheric winds
  - QBOWM: Westerly mid-stratospheric winds

## Result: MJO-QBO Relationship

### QBO and Lower-Stratospheric Stability

**Primary Result 2:** During winter, QBO winds drive stability changes in the lower stratosphere that correspond to stronger MJO events propagating across the MC. The impact of these QBO-driven stratospheric zonal winds on lower-stratospheric stability and MJO depends on the altitude of those winds, as well as their direction and speed.

During boreal winter, zonal wind shear is in thermal wind balance with stratospheric temperature anomalies.

$$\frac{du}{dz} = -\frac{R}{H\beta} \frac{\delta^2 T}{\delta y^2} \Rightarrow \frac{du}{dz} \propto T' \quad (2)$$

During winter, temperature anomalies ( $T'$ ) are proportional to zonal wind shear ( $du/dz$ ) (Fig. 8, Eq. 2; (Holton and Hakim, 2013)).

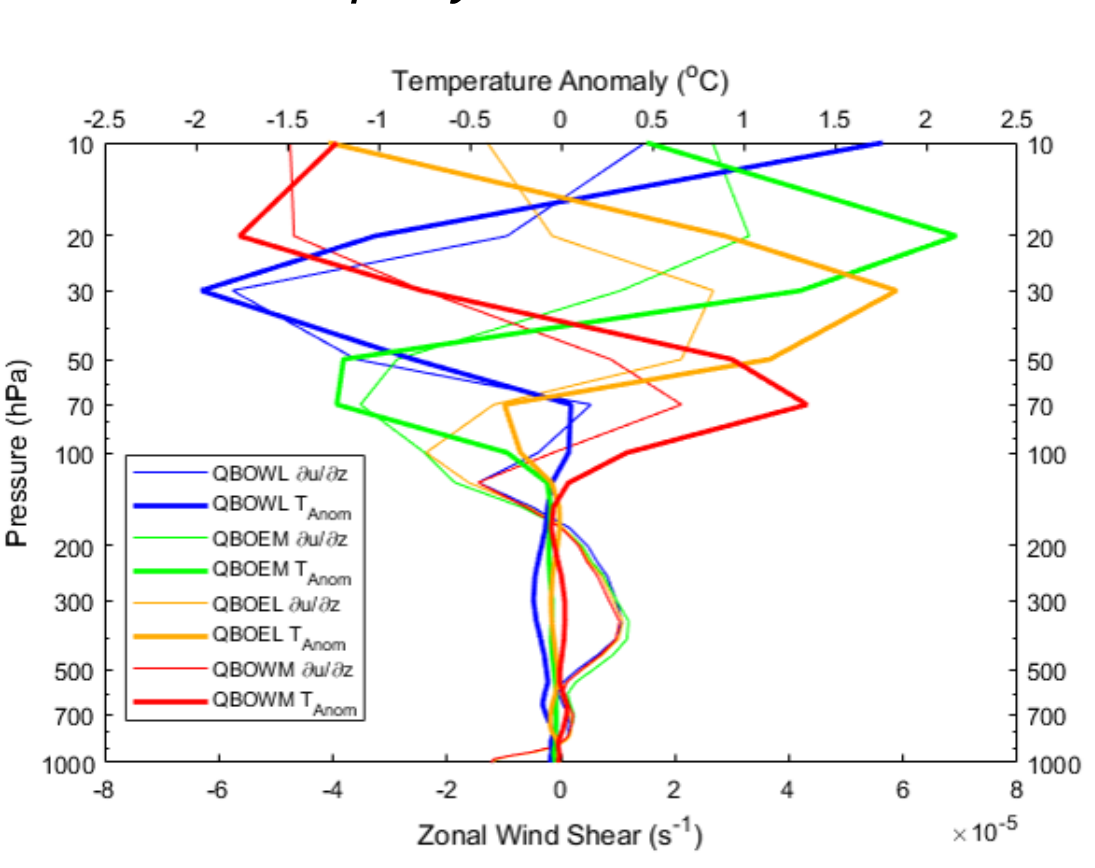


Figure 8: Zonal wind shear values (thin lines) and temperature anomalies (thick lines) associated with each of the four QBO phase pairs.

Changes in zonal winds with height therefore create warm and cold temperature anomalies in the stratosphere.

These temperature changes drive stability changes which can either enhance or weaken high-altitude thunderstorm activity associated with the MJO.

### QBO and MJO Amplitude Change by Season

**Primary Result 3:** MJO propagation exhibits a statistically significant relationship with QBO that reverses with season. In northern hemisphere winter, MJO events strengthen over the MC when mid-stratospheric winds are easterly and weaken when those winds are westerly. During northern hemisphere spring and summer, MJO and BSISO events weaken more when mid-stratospheric winds are easterly.

The relationship between QBO and MJO propagation over the MC is significant and reverses with season.

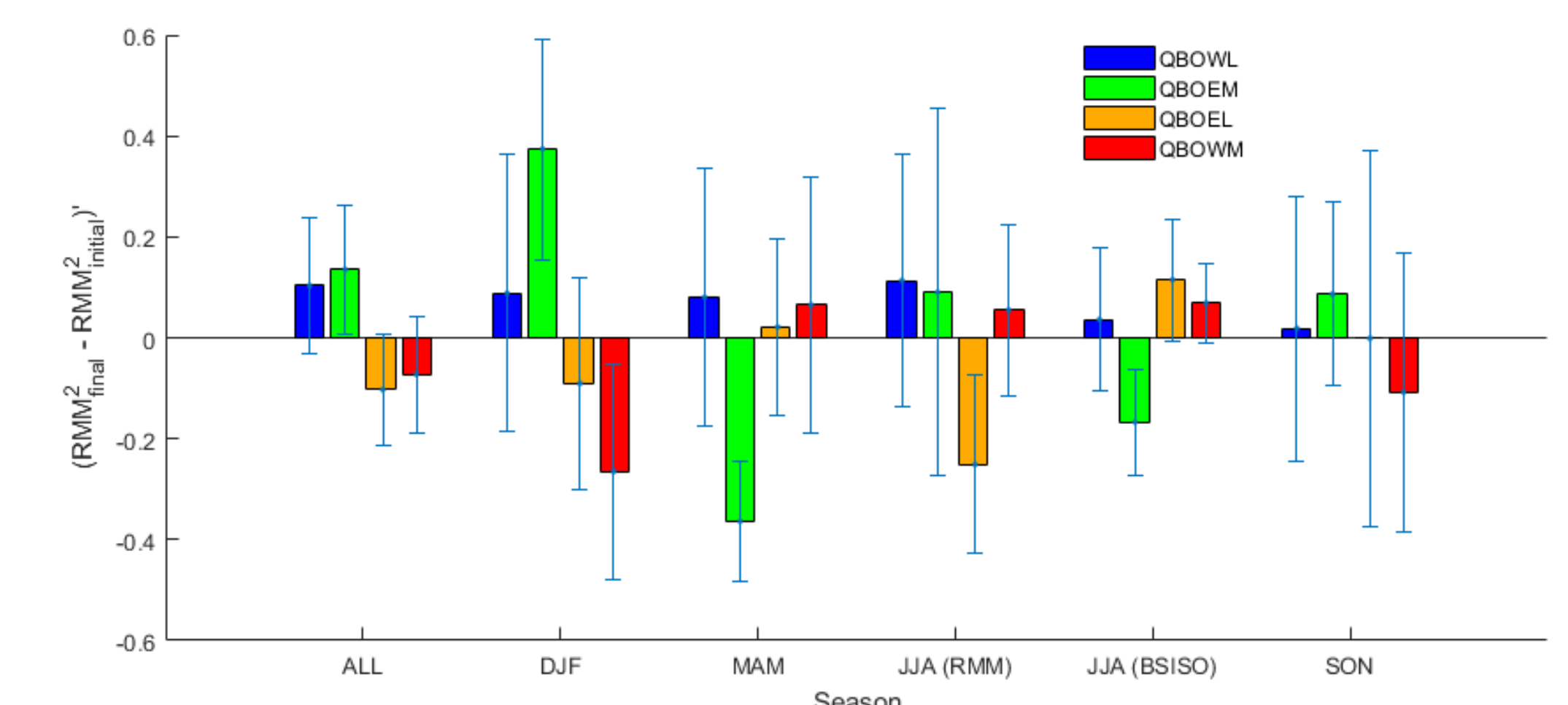


Figure 9: Mean amplitude change difference from climatological (1980-2017) average for initially active MJO events, binned by QBO phase pair and seasonal subset. Boreal summer (JJA) analysis is repeated using MJO RMM amplitudes and BSISO amplitudes.

### Winter (December-February)

- QBOEM: MJO **strengthens** over the MC
  - Easterly zonal wind shear cools the lower stratosphere, lowering lower stratospheric stability and enhancing deep convection associated with the MJO (Fig. 10)
- QBOWM: MJO **weakens** over the MC
  - Westerly zonal wind shear heats the lower stratosphere, increasing lower stratospheric stability and weakening deep convection associated with the MJO (Fig. 10)
- QBOWL and QBOEL: no significant change occurs

### Spring (March-May)

- QBOEM: MJO **weakens** over the MC
- All other phase pairs: no significant change occurs

### Summer (June-August)

- RMM Index: No significant change in MJO by QBO phase
- BSISO Index:
  - QBOEM: BSISO **weakens** over the MC
  - All other phase pairs: no significant change occurs

Some of this seasonal reversal may be due to seasonal differences in 100 hPa stability (not shown):

- QBOEM and QBOWM stability anomalies are diminished during MAMJJA
- Mechanisms which could explain the spring and summer relationship are recommended for further study

## Quasi-Biennial Oscillation (QBO) and MJO

Other atmospheric oscillations can project onto weather patterns with shorter timescales, including the MJO. Previous studies have linked MJO amplitude to the polarity of one such interannual oscillation: the Quasi-Biennial Oscillation (QBO; e.g. Son et al. 2017).

The QBO consists of alternating centers of easterly and westerly winds descending through the equatorial stratosphere. These winds may affect MJO propagation (Fig. 3).

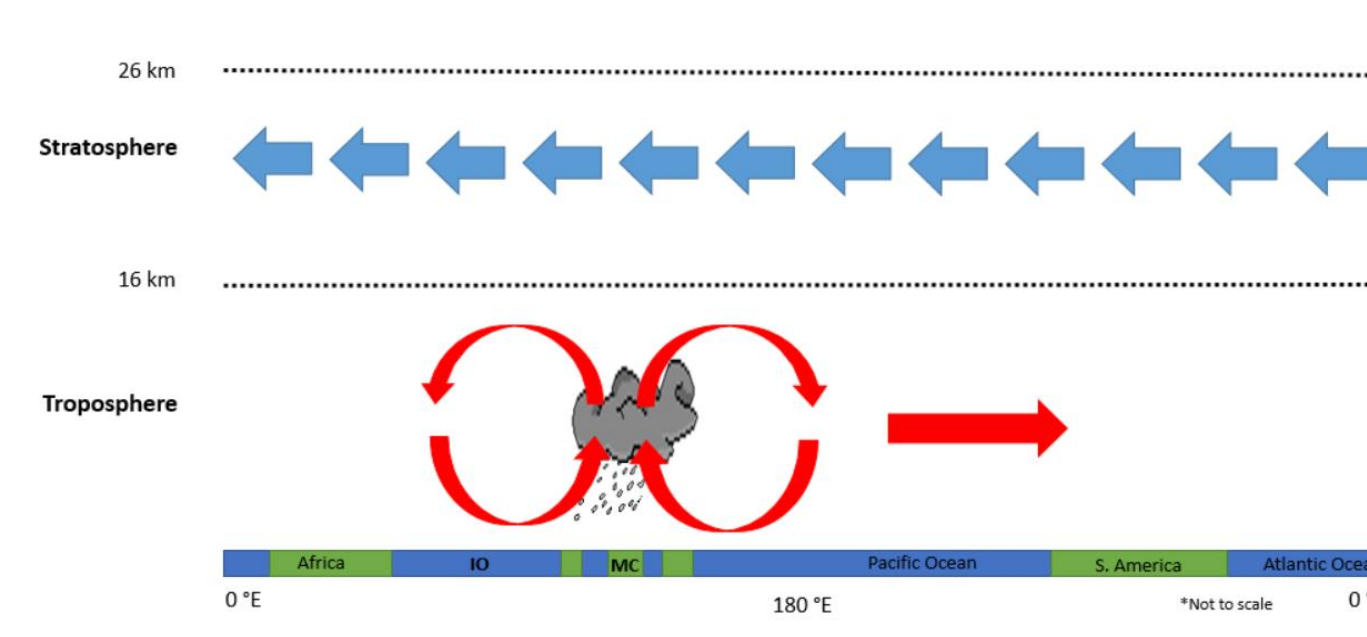


Figure 3: Zonal winds associated with the QBO (blue arrows) represent zonal flow associated with the easterly QBO polarity relative to MJO atmospheric circulation and convection (represented by the red arrows and cloud).

## Works Cited

Dee, D.P. and Coauthors, 2011: The ERA-Interim reanalysis: configuration and performance of the data assimilation system. *Quart. J. Roy. Meteor. Soc.*, 137, 553-597, doi:10.1002/qj.828

Department of Defense, Summary of the 2018 National Defense Strategy of the United States of America, *Defense.gov*, doi:10.1002/qj.828

Feng, J., T. Li, and W. Zhu, 2015: Propagating and nonpropagating MJO events over Maritime Continent. *J. Climate*, 28, 8430-8449, doi:10.1175/JCLI-D-15-0085.1

Holton, J. R., and G. J. Hakim, 2013: *An Introduction to Dynamic Meteorology*, 3rd Edition, Academic Press, 532 pp.

Inness, P. M., and J. M. Slingo, 2006: Simulation of the Madden-Julian Oscillation in a coupled general circulation model. *J. Climate*, 19, 1645-1667, doi:10.1175/JCLI1515-1159.1

Kikuchi, G., B. Wang, and Y. Kajikawa, 2012: Bimodal representation of the tropical intraseasonal oscillation. *Climate Dyn.*, 38, 1989-2000, doi:10.1007/s00382-011-1159-1

Kiladis, G. N., J. Diaz, K. H. Straub, M. C. Wheeler, S. N. Tulich, K. Kikuchi, K. M., Weickmann, and M. J. Ventrice, 2014: A comparison of OLR and circulation-based indices for tracking the MJO. *Mon. Wea. Rev.*, 142, 1697-1715, doi:10.1175/MWR-D-13-00301.1

Lee, J., B. Wang, M. C. Wheeler, X. Fu, D. E. Waliser, and S. Kang, 2013: Real-time multivariate indices for the boreal summer intraseasonal oscillation over the Asian summer monsoon region. *Climate Dyn.*, 40, 493-509, doi:10.1007/s00382-012-1554-4

Madden, R. A., and P. R. Julian, 1971: Detection of a 40-50 day oscillation in the zonal wind in the tropical Pacific. *J. Atmos. Sci.*, 28, 702-708, doi:10.1175/1520-0469(1971)028<702:MO>2.0.CO;2

Madden, R. A., and P. R. Julian, 1994: Observations of the 40-50 day tropical oscillation: a review. *Mon. Wea. Rev.*, 122, 814-836, doi:10.1175/1520-0493(1994)122<0814:OOA>2.0.CO;2

Son, S., Y. Lim, C. Yoo, H. Hendon and J. Kim: Stratospheric control of the Madden-Julian Oscillation. *J. Climate*, 20, 1909-1922, doi:10.1175/JCLI-D-16-0620.1

Speicher, K., 2003: Propagation and the vertical structure of the Madden-Julian Oscillation. *Mon. Wea. Rev.*, 131, 3018-3037, doi:10.1175/1520-0493(2003)131<3018:POV>2.0.CO;2

Wheeler, M., and H. Hendon, 2004: An all-season real-time multivariate MJO index: Development of an index for monitoring and prediction. *Mon. Wea. Rev.*, 132, 1917-1932, doi:10.1175/1520-0493(2004)132<1917:AMJO>2.0.CO;2

Zhang, C., 2005: Madden-Julian Oscillation. *Rev. Geophys.*, 43, doi:10.1029/2004RG000158

**Acknowledgements:** The authors gratefully acknowledge the support of ONR award N0001416WX01752 and the USNA Midshipman Research Office.

## Military Relevance

MJO strength and propagation across the MC is affected by:

- Initial strength and moisture in the MJO active envelope
- Surface conditions over the MC
- Zonal stratospheric winds above the MJO active envelope

Naval operations and interests near the Maritime Continent are related to the 2018 National Defense Strategy:

- Straits of Malacca: a critical sea lane for US Navy transit to 5th Fleet
- South China Sea: a region of growing US strategic interest

### Impacts:

- The greatest operational impact of the MJO is **severe weather associated with thunderstorms**. Ensuring high winds, reduced visibility, lightning and other hazards preclude normal operations.
- These results **improve the ability to anticipate these adverse conditions**, which can improve mission planning and effectiveness.



Figure 11: Top: USS LASSEN, one of several US Navy vessels to conduct a freedom of navigation pass in the South China Sea. Bottom: One of the Spratly Islands, in the South China Sea.